Renewable Energy 68 (2014) 893–905

Contents lists available at ScienceDirect

Renewable Energy

journal homepage: www.elsevier.com/locate/renene

Multidisciplinary design optimization of offshore wind turbines for minimum levelized cost of energy

T. Ashuri [a,*], M.B. Zaaijer [b], J.R.R.A. Martins [a], G.J.W. van Bussel [b], G.A.M. van Kuik [b]

[a] University of Michigan, Department of Aerospace Engineering, Ann Arbor, MI 48109, USA
[b] Delft University of Technology, Department of Aerodynamics and Wind Energy, Kluyverweg 1, 2629 HS Delft, The Netherlands

ARTICLE INFO

Article history:
Received 2 February 2013
Accepted 25 February 2014
Available online 21 March 2014

Keywords:
Offshore wind turbine
Multidisciplinary design optimization
Aeroelasticity
Rotor design
Tower design
Levelized cost of energy

ABSTRACT

This paper presents a method for multidisciplinary design optimization of offshore wind turbines at system level. The formulation and implementation that enable the integrated aerodynamic and structural design of the rotor and tower simultaneously are detailed. The objective function to be minimized is the levelized cost of energy. The model includes various design constraints: stresses, deflections, modal frequencies and fatigue limits along different stations of the blade and tower. The rotor design variables are: chord and twist distribution, blade length, rated rotational speed and structural thicknesses along the span. The tower design variables are: tower thickness and diameter distribution, as well as the tower height. For the other wind turbine components, a representative mass model is used to include their dynamic interactions in the system. To calculate the system costs, representative cost models of a wind turbine located in an offshore wind farm are used. To show the potential of the method and to verify its usefulness, the 5 MW NREL wind turbine is used as a case study. The result of the design optimization process shows 2.3% decrease in the levelized cost of energy for a representative Dutch site, while satisfying all the design constraints.

1. Introduction

Due to concerns over the environmental impact of fossil fuel emissions and fossil fuel exhaustion, the amount of wind energy generated has been increasing at a faster pace in the last few years. Although wind energy has evolved considerably during the last decades, there are many advances required to design economic and reliable wind turbines.

One of the promising concepts that can contribute to these goals is the use of multidisciplinary design optimization (MDO). MDO uses numerical optimization techniques to design engineering systems involving multiple disciplines or components Martins and Lambe [1].

In the context of wind power design optimization two subjects are of interest: the design optimization of wind turbines and wind farm layout optimization.[1] The scope of this paper is wind turbine design optimization considering aerodynamics and structure as the two main disciplines, with the simultaneous design of the rotor and tower as the two main components.

Over the past decade, several authors have developed techniques for optimizing either the rotor or tower, with most of the studies being focused on rotor optimization. A brief overview of these studies is presented below.

1.1. Rotor design studies

A method for optimizing wind turbine gross parameters, such as rotor diameter and hub height for a specific site was presented by Diveux et al. [9]. Similarly, Fuglsang and Thomsen [10] conducted rotor design optimization with several site-specific environmental inputs to minimize the cost of energy (COE). Benini and Toffolo [11] used a multi-objective evolutionary algorithm to optimize the aerodynamic shape of a stall-regulated wind turbine blade.

Maalawi and Negm [12] presented an optimization study to make an exact placement of natural frequencies of the blade to avoid resonance. Maalawi and Badr [13] optimized the rotor chord and twist to produce the largest possible power output. Jureczko et al. [14] studied the blade structural lay-up optimization to minimize its mass.

* Corresponding author.
E-mail address: tashuri@umich.edu (T. Ashuri).

[1] For wind farm layout optimization the interested reader can consult various references Beyer et al. [2], Grady et al. [3], Castro Mora et al. [4], Marmidis et al. [5], Kusiak and Song [6], Emami and Noghreh [7], Meyers and Meneveau [8].

http://dx.doi.org/10.1016/j.renene.2014.02.045
0960-1481/

The blade structural optimization of laminated composite shells was studied by Lund and Stegmann [15]. The shape and thickness of the structure were fixed and the problem dealt entirely with the design of the lay-up of the composite laminate. Méndez and Greiner [16] used a genetic algorithm to obtain optimal chord and twist distributions in wind turbine blades to maximize the mean expected power depending on the Weibull wind distribution at a specific site. Lee et al. [17] studied blade shape optimization to obtain the maximum average annual power for a given offshore wind farm. A two-step optimization procedure was established: the operating condition optimization as step one, and the geometric blade shape design and blade performance analysis optimization as step two.

Kenway and Martins [18] studied the blade aerostructural design optimization to maximize the energy output while considering site-specific winds. Xudong et al. [19] used an aeroelastic model of the rotor to do aerodynamic and structural design with the rotor torque and thrust as the design constraints.

Blade aerodynamic shape optimization using different tip-loss corrections in blade element momentum (BEM) theory was studied by Clifton-Smith [20]. The blade aerodynamic shape optimization with a probabilistic approach was studied by Lee et al. [21].

To enhance the aerodynamic performance of blades, the sectional aerodynamic design optimization was studied by Kwon et al. [22]. Design optimization of a wind turbine blade was presented by Jeong et al. [23] to minimize the fluctuation of the bending moment of the blade in turbulent wind.

Blade structural and aerodynamic optimization was presented by Bottasso et al. [24]. Design optimization is performed by a two-stage process. First, an aerodynamic shape optimization step is performed to maximize annual energy production (AEP), followed by a structural blade optimization to minimize weight. Second, both designs are combined to yield the final optimum solution.

The system-level design of a wind turbine blade using a multi-level optimization approach was studied by Maki et al. [25]. The shape optimization of the blade to maximize AEP, and the structural design of the blade to minimize the bending moment at the root were considered as single-disciplinary optimization strategy. Cost of energy was considered as the overall system-level objective, while performance improvements at the two single-disciplines were pursued at the same time.

1.2. Tower design studies

Negm and Maalawi [26] examined several optimization models such as mass reduction, stiffness maximization and vibration minimization for the design of a tubular wind turbine tower structures. Wind turbine tower optimization was studied by Yoshida [27] using a genetic algorithm to minimize the mass of the tower. Uys et al. [28] developed a procedure to minimize the cost of a mildly conical steel wind turbine tower to meet the structural requirements of slender structures.

A formulation for the optimal design of reinforced concrete towers was presented by Silva et al. [29]. Different tower heights were analyzed to obtain the best formulation in terms of cost. An integrated reliability-based design optimization of offshore towers was presented by Karadeniz et al. [30]. As a demonstration, they optimized a tripod tower subject to reliability constraints based on limit states of the critical stress, buckling and the natural frequency.

Similarly, Petrini et al. [31] proposed a system approach as a conceptual method for the design of offshore wind turbine structures. Numerical analysis has been performed to compare the design of three different support structure types (monopile, tripod and jacket) with respect to extreme loads, buckling, natural frequencies and life-time loads.

Torcinaro et al. [32] considered the optimization process of an offshore support structure intended for a 5–6 MW turbine. Support structure geometry and thickness were the design variables subjected to constraints on stresses, buckling and deformation. Mass is optimized using gradient based optimization algorithm.

Thiry et al. [33] used a genetic algorithm to minimize the structural weight of a wind turbine support structure for an offshore application. Haghi et al. [34] used a similar approach, but instead of using a genetic algorithm he used gradient-based optimization. Zwick et al. [35] presented an iterative optimization approach for a first stage of a complete analysis of a full-height lattice tower concept. The aim was to find a light-weight design to fulfill the ultimate and fatigue limit states of the members.

Molde [36] used Spall's simultaneous perturbation stochastic approximation method Spall [37] to automatically optimize thickness and diameter of the members in offshore lattice tower support structures. The objective was to minimize tower weight. Karpat [38] minimized the cost of wind turbine steel towers with ring stiffeners using a particle swarm optimization algorithm. The height and thickness of a flat ring stiffener, and the wall thickness and the diameter at some stations along the tower were selected as the design variables, subject to buckling and frequency constraints.

The work presented herein addresses some of the shortcomings of the previous work mentioned above by developing an integrated MDO method to simultaneously design the rotor and the tower of a wind turbine at the system level. The design found in this way is superior to the design found by optimizing each discipline or component separately, since MDO of the rotor and tower incorporates the dynamic interaction between the disciplines and components. This interaction is particularly important, due to the following factors:

1.2.1. Structural flexibility

Rotor and tower are the most flexible components of a wind turbine, and together they dominate the global dynamics of the system.

1.2.2. Energy yield

Rotor and tower (also the controller) have the highest impact on the annual energy yield of the wind turbine, therefore important to optimize simultaneously.

1.2.3. Cost

Rotor and tower (also the gearbox) have the highest cost share of a wind turbine. Typically, rotor and tower make up to 30% of the capital cost of a wind turbine Tegen et al. [39].

The remainder of the paper is structured as follows. First, the integrated architecture used to model the multidisciplinary aspects of the wind turbine is presented. This is an important aspect, since existing computational tools are not well suited to be used with numerical optimization that is fully automated.[2]

We then describe how this integrated multidisciplinary model is linked to the optimization algorithm. This enables running the design optimization process for as many iterations as the optimizer needs to find the optimum. Then, to verify the capability and effectiveness of the method, the 5 MW NREL research wind turbine Jonkman et al. [41] is used as a baseline design to optimize. Both the rotor and tower are designed simultaneously with all their relevant design constraints present. Finally, the results of the optimized 5 MW turbine are compared with the 5 MW NREL wind turbine, followed by a discussion and conclusions.

[2] See Ashuri and Zaaijer [40] for a list of the main computational tools currently used for wind turbine design.

2. Methodology

Among the several MDO architectures described in the literature, this study implements the multidisciplinary feasible (MDF) architecture explained by Martins and Lambe [1]. In the next subsection we describe how MDF is implemented, including the details of how the various models are coupled and how the overall optimization process is sequenced.

2.1. MDO architecture

With the MDF architecture, the idea is to directly couple an optimizer to a multidisciplinary analysis model, as shown in Fig. 1. We use the extended design structure matrix (XDSM) standard developed by Lambe and Martins [42] for the diagram. The aerodynamic and structural design variables are passed to the multidisciplinary analysis, which computes the objective function and constraints for the coupled system. Then, the objective and constraints are passed back to be assessed by the optimizer. This iterative approach continues until the convergence is achieved.

To compute the objective function and design constraints, a multidisciplinary analysis is required that couples the computational tools representing the various disciplines involved. Among the many computational tools that have been developed for the wind energy community, a number of NREL tools are used, and they are listed in Table 1. These tools are all open source, which makes them particularly well suited for research purposes.

The computational tools listed in Table 1 are in principle independent and not designed with coupling in mind. Thus, the data transfer between these codes has to be done manually by the designer. To make an integrated and automated design process, we coupled these computational tools such that the final product could be easily linked with optimization software using the MDF architecture.

Fig. 2 shows how the tools are coupled in a framework that captures the static and dynamic behavior of the wind turbine, and evaluates the design constraints and objective function. This integration is achieved by a script that manages the data flow between all the codes. The script is used to manage the design optimization process such that:

1. The coupling of different tools is effective and yields the correct result.
2. All data exchanges are automatic.
3. All design changes are reflected in the relevant locations in the framework.

Table 1
Selection of the computational tools.

Tool	Usage	Reference
TurbSim	Simulates the 3D turbulent wind flow	Jonkman and Buhl [43]
AeroDyn	Models the steady and unsteady aerodynamic loads	Laino and Hansen [44]
AirfoilPrep	Corrects 2D airfoil data for 3D effects	Viterna and Janetzke [45]
FAST	Models the aeroelastic behavior of the wind turbine	Jonkman and Buhl [46]
BModes	Computes mode shapes and frequencies	Bir [47]
Crunch	Postprocesses the FAST output data	Buhl [48]
Cost-mass models	Computes mass and cost of components	Fingersh et al. [49]
Fatigue	Computes rain-flow cycle counted time series	Frendahl and Rychlik [50]

2.2. Optimization problem formulation

In order to solve the correct design problem, we must define the optimization problem with the appropriate objective, design variable and design constraints. The general nonlinear optimization problem is:

$$\text{Find } x = \{x_1, \ldots, x_n\} \text{that minimizes } f(x) \tag{1}$$

where f is the objective function, and x is an n-dimensional vector of design variables to be found, with lower and upper bounds:

$$x_{\text{lower}} \leq x \leq x_{\text{upper}} \tag{2}$$

The problem is subject to inequality and equality constraints:

$$g_j\{x\} \geq 0 \tag{3}$$

$$h_k(x) = 0 \tag{4}$$

We now describe what these general terms are in the specific case of the wind turbine problem that we solve.

2.2.1. Design variables

A design variable is a parameter that the optimizer controls, whose influence on the constraints and objective function is evaluated in the analysis phase. In this paper, the rotor optimization controls 18 design variables that consist of blade external geometry variables, blade structural thickness variables and rotor rotational speed. The blade geometry variables are 4 chord lengths, 2 twists

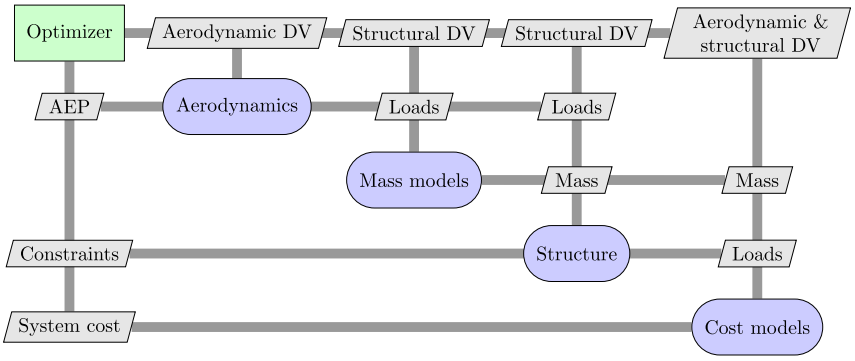

Fig. 1. Multidisciplinary feasible architecture to couple the optimizer to the multidisciplinary analysis model. Green box is the optimizer, rounded blue boxes are the analysis models, gray parallelograms are data (design variables (DV), loads, mass, costs, annual energy production (AEP) and constraints) and gray lines show the data flow that is from top to bottom and left to right on the upper triangular part, and bottom to top and right to left on the lower triangular part. Table 2 lists the aerodynamic and structural design variables shown in this figure. (For interpretation of the references to color in this figure legend, the reader is referred to the web version of this article.)

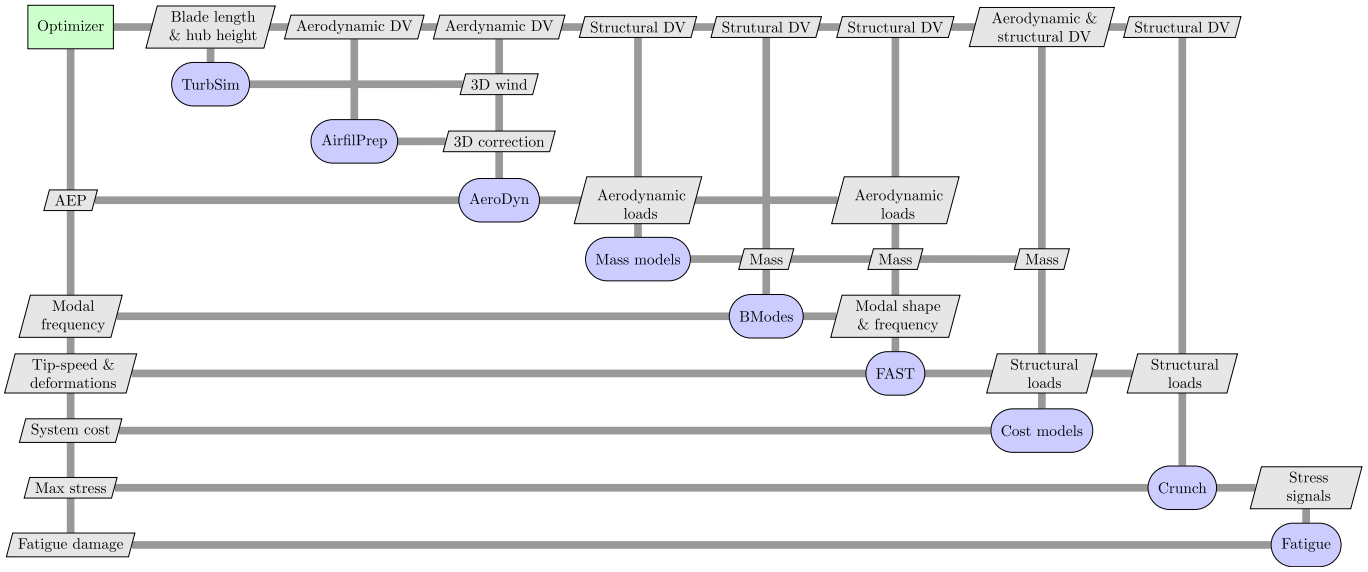

Fig. 2. Block diagram of the MDO framework to show the data and process flow of different computational codes. Table 2 lists the aerodynamic and structural design variables shown in this figure. Green box is the optimizer, rounded blue boxes are the analysis models, gray parallelograms are data, and gray lines show the data flow that is from top to bottom and left to right on the upper triangular part, and bottom to top and right to left on the lower triangular part. (For interpretation of the references to color in this figure legend, the reader is referred to the web version of this article.)

along the span and blade length. The structural thicknesses of the composite lay-ups are spar thicknesses at 3 stations, shell thicknesses at 4 stations, and web thicknesses at 3 stations along the blade. The rotational speed of the rotor together with the blade length control the tip-speed of the blade, which is a crucial design constraint.

The optimization of the tower controls 5 design variables: tower diameter at the bottom (interface) and top (connection to nacelle), tower thickness at the bottom and top, and tower height. Table 2 lists the design variables of the blade and tower, and their upper and lower bounds.

Similar to the NREL 5 MW offshore tower, the tower in this work starts from the interface level and extends up to the bottom of the nacelle. Therefore, it is only the tower that is optimized up to the interface level and mass and cost models are used for below interface level (for transition piece, and monopile) based on the WindPACT study Fingersh et al. [49].

As long as there is not a significant change of the turbine properties, environmental condition such as water depth, and the rated power is kept constant this assumption is acceptable. However, this becomes invalid when significant changes are made to the design or environmental conditions, and these models need to be tuned to cope with these changes. Also, the pile–soil interaction is not considered in this work, to make a meaningful comparison between the baseline and optimized 5 MW turbines.

Fig. 3 shows different stations along the blade and tower. All these design variables are continuous, and they are defined several stations along the blade and tower. A combination of linear and cubic interpolations are used to define the values at intermediate stations along the blade and tower. Additionally, because of the complex geometry and composite layup of the blade, the following parameters are fixed to control and enable a smooth interpolation of the design variables:

1. Stations 1 to 3 have a circular cross section and all three stations have the same diameter.
2. The structural chord at station 20 is set to 0.12 cm (similar to the NREL case). A cubic interpolation is used from station 3 to the tip.
3. Structural twist from stations 1 to 6 is set to 13.1 deg (similar to the NREL case). A cubic interpolation is used from station 6 to 9, followed by a linear interpolation from station 9 to the tip.
4. Structural twist at the blade tip is set to 0 deg (similar to the NREL case).
5. The shear web and cap thicknesses at station 1 are 0 cm. A cubic interpolation is used from the blade root to the tip.

2.2.2. Design constraints

In addition to the design variable bounds listed in Table 2, several functional design constraints are enforced. Design constraints are in general nonlinear functions that must be satisfied in an optimization problem. A total of 51 inequality constraints are enforced in the optimization of the rotor and tower. Partial safety

Table 2
5 MW wind turbine design variables and their bounds.

Index	Description (units)	Min	Max	Discipline
1	Blade length (m)	56.0	65.0	Structure
2	Tower height (m)	78.5	95.0	Structure
3	Rated rotational speed (rpm)	10.5	13.4	Aerodynamics
4	Twist at station 9 (deg)	9.0	14.0	Aerodynamics
5	Twist at station 15 (deg)	1.0	4.0	Aerodynamics
6	Chord at station 3 (m)	3.0	4.0	Aerodynamics
7	Chord at station 7 (m)	4.0	5.5	Aerodynamics
8	Chord at station 15 (m)	2.1	3.0	Aerodynamics
9	Chord at station 18 (m)	1.3	2.3	Aerodynamics
10	Skin thickness at station 1 (cm)	8.0	14.0	Structure
11	Skin thickness at station 3 (cm)	5.0	10.0	Structure
12	Skin thickness at station 6 (cm)	2.0	5.0	Structure
13	Skin thickness at station 16 (cm)	1.0	4.0	Structure
14	Web thickness at station 3 (cm)	1.0	5.0	Structure
15	Web thickness at station 6 (cm)	2.0	4.0	Structure
16	Web thickness at station 16 (cm)	1.0	3.0	Structure
17	Spar thickness at station 3 (cm)	1.0	4.0	Structure
18	Spar thickness at station 6 (cm)	1.0	4.0	Structure
19	Spar thickness at station 16 (cm)	1.0	4.0	Structure
20	Tower diameter at station 1 (m)	4.0	7.0	Structure
21	Tower diameter at station 22 (m)	3.0	5.0	Structure
22	Tower thickness at station 1 (cm)	4.0	6.0	Structure
23	Tower thickness at station 22 (cm)	2.0	5.0	Structure

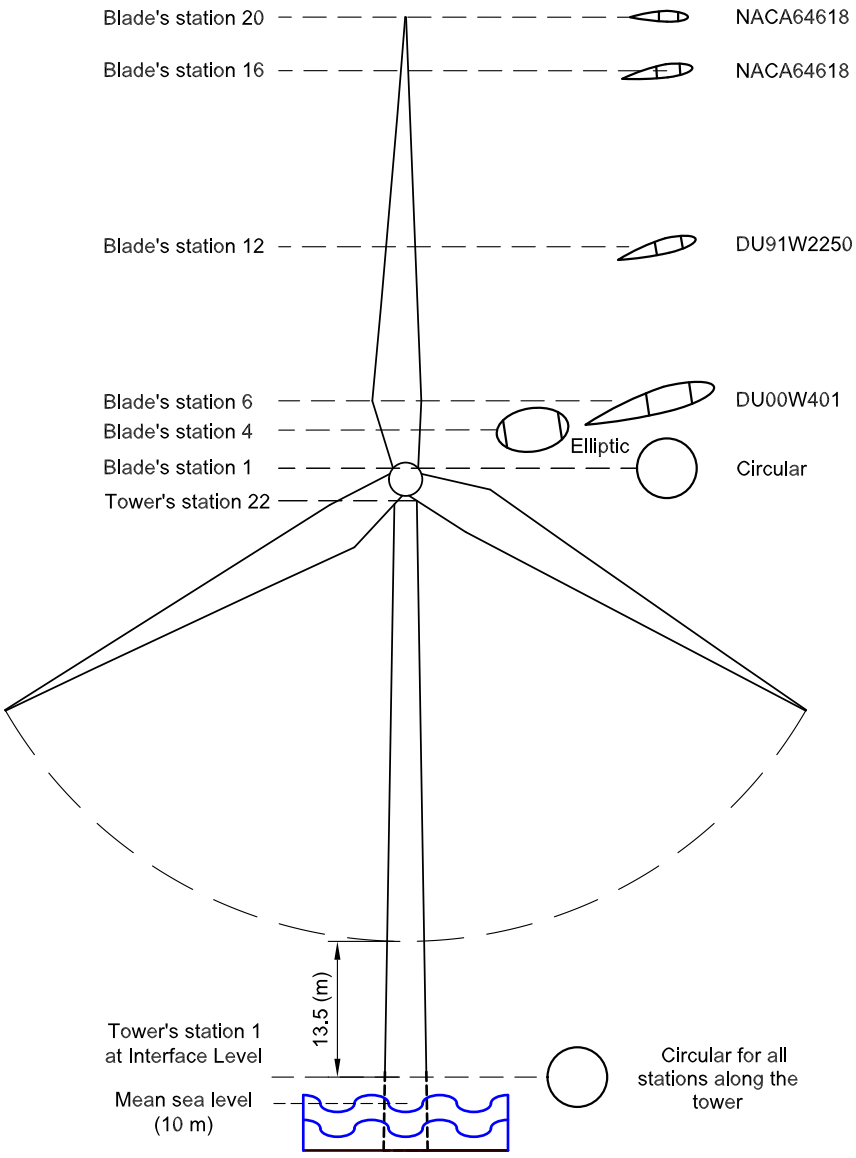

Fig. 3. Different stations along the blade and tower to show the geometry and the approximate location of each station. Station 1 of the blade defines the root and station 20 the tip. Station 1 of the tower defines the interface level and station 22 the tower top.

factors (as prescribed by IEC61400 [51]) are also included in these design constraints.

The blade constraints are: stresses and fatigue damage (fatigue damage calculation is done using rain flow cycle counting of the stress time-signals and applying Palmgren-Miner's rule Miner [52]) at 5 stations along the blade, tip-deflections from 9 to 25 m/s with 2 m/s interval, and the first 3 natural frequencies. Table 3 lists the design constraints of the blade.

The tower design constraints are: stresses and fatigue damage at 6 stations along the tower, and the first two natural frequencies. Table 4 list the design constraints for the tower. All the design constraints of the blade and tower are continuous, smooth and differentiable.

Fatigue properties are determined by the slope of the S–N curves, and the location of the intercept with the abscissa. For the composite blade, a slope of 10 and an intercept of 40 MPa is used. For the steel tower, a slope of 4 and an intercept of 110 MPa is used.

Table 3
Wind turbine blade design constraints.

Index	Description	Value (units)
1–9	Max flapwise tip-deflection from 9 to 25 m/s	≤5.6 (m)
10–15	Max flapwise fatigue at stations 1, 3, 7, 10, 12 and 14	≤0.7 (–)
16–21	Max edgewise fatigue at stations 1, 3, 7, 10, 12 and 14	≤0.7 (–)
22–27	Max flapwise stress at stations 1, 3, 7, 10, 12 and 14	≤200 (MPa)
28–33	Max edgewise stress at stations 1, 3, 7, 10, 12 and 14	≤200 (MPa)
34–36	1st to 3rd natural frequency	≤0.7 (Hz)
37	Tip-speed	≤120 (m/s)

2.2.3. *Objective function*

When applying any changes to a given design, it is important to know the influence of this change at the system level. For example, an increase in blade length to increase AEP increases

Table 4
Wind turbine tower design constraints.

Index	Description	Value (units)
1–6	Fore-aft stress at stations 1, 5, 9, 13, 17 and 21	≤150 (MPa)
7–12	Fore-aft fatigue at stations 1, 5, 9, 13, 17 and 21	≤0.7 (–)
13–14	1st and 2nd natural frequency of the tower	$0.3 \leq \omega_{2n} \leq 0.56$ (Hz)

loads and installation costs. If one effect does not balance out the other, then the proposed change might result in a negative overall impact.

Since the design optimization is carried out at the system level instead of the component level, and the mass of all the NREL wind turbine components is not defined, mass models are used to represent the global dynamics of all components of the wind turbine (except for the rotor and tower, which are directly optimized). In addition, instead of using a single-disciplinary objective function such as AEP (aerodynamics) or load-mass (structures), the levelized cost of energy (LCOE) is used as a multidisciplinary objective function.

The LCOE is a good objective function because it reflects the overall goal of wind energy production, and it also accounts for all the multidisciplinary trade-offs when a coupled analysis is performed at the system-level Ashuri [53].

LCOE is a continuous, smooth and differentiable function, which enables the use of gradient-based optimization algorithms. To make a realistic estimation of the LCOE, it is assumed that all the cost elements correspond to a wind turbine that operates in an offshore farm. These cost elements are explained by Fingersh et al. [49], and the details are not repeated here. The LCOE covers the following items:

2.2.3.1. Turbine capital cost (TCC). This is the cost of all the components of a wind turbine. These are: blades, hub, pitch mechanism and bearings, nose cone, low speed shaft and bearings, gearbox, mechanical brake, high speed shaft and coupling, generator, power electronics, yaw drive and bearing, main frame, electrical connections, hydraulic system, cooling system, nacelle cover, control equipment, safety system, condition monitoring, tower, marinization (extra cost to protect against marine environment like salty water).

2.2.3.2. Balance of station (BOS). This is the cost of following items: monopile, port and staging equipment, turbine installation, electrical interface and connections, permits, engineering, site assessment, personnel access equipment, scour protection, transportation, offshore warranty premium and decommissioning.

2.2.3.3. Initial capital cost (ICC). Summation of the TCC and BOS costs.

2.2.3.4. Levelized replacement cost (LRC). This is the cost of major replacements and overhauls, distributed over the life time of the wind turbine.

2.2.3.5. Operations and maintenance (O&M). Cost associated to fix failures of mechanical or electrical components and all the regular and irregular inspection of the wind turbine.

LCOE is calculated using the following equation:

$$\mathrm{LCOE} = \left(\frac{(\mathrm{ICC}\times\mathrm{FCR})+\mathrm{LRC}+\mathrm{O\&M}}{\mathrm{AEP}}\right) \tag{5}$$

here, FCR is the Fixed Charge Rate, which includes construction financing, financing fees, return on debt and equity, depreciation, income tax, and property tax and insurance. AEP is the amount of generated electricity in a year for a given wind speed distribution $f(V)$,. It also includes the mechanical and electrical conversion losses, and machine availability. The wind speed distribution is given by the Weibull distribution:

Table 5
Definition of DLCs based on IEC standard.

Design situation	Design load case	Simulated wind (m/s)	Wind-wave misalignment	Analysis type
Power production	1.2	4 to 25	Aligned	Fatigue
Parked	6.1	50	Aligned	Ultimate

$$f(V) = \left(\frac{k}{c}\right)\left(\frac{V}{c}\right)^{k-1}\exp\left[-\left(\frac{V}{c}\right)^{k}\right] \tag{6}$$

where V is the wind velocity, k is the shape factor, and c the scale factor. In this paper, k is 2, and c is 9.47. These values typically represent the condition of the Dutch part of the North Sea Brand [54]. Then, the AEP production can be expressed as:

$$\mathrm{AEP}\approx 8760\times\sum_{i=\mathrm{cut-in}}^{\mathrm{cut-out}} P(V_i)\cdot f(V_i) \tag{7}$$

in which 8760 is the number of hours per year $P(V)$, is the power curve of the wind turbine, and the index i represents the discretized wind speed with a bin interval of 2, i.e. 5, 7, …, 25.

However, these cost models were calibrated based on 2002 costs and should be updated based on the cost of materials and products in the present time to account for the inflation of materials, products and labor. To compensate for this difference, a component cost escalation model based on the Producer Price Index (PPI) is used, as recommended by the WindPACT study. The PPI is an index that is updated on a monthly basis by the US Department of Labor, Bureau of Labor Statistics, to track the changes of costs of products and materials over a wide range of industries and industrial products. The PPI related formulas are sorted by North American Industry Classification System (NAICS) codes that provide a grouping system of products.[3]

2.2.4. External condition and design load case (DLC)

An estimate of the loading conditions that a wind turbine experiences in its lifetime must be analyzed. For this estimate the IEC 61400-3 standard is used, where the external conditions are site dependent and wind turbine classes are defined in terms of wind speed and turbulence parameters at hub-height with a reference period of 630 s (the first 30 s is ignored to avoid strange transient behavior) for each random seed. This paper uses the 2009 edition of IEC 61400-3 standard for defining the design load cases, and based on Section 7.4 of this standard, the design load cases used for simulations are defined in Table 5. The IEC-1B class is used for these load cases.

For the fatigue limit state, a Normal Turbulence Model (NTM) during the power production mode is used. This model is applied from the cut-in to cut-out wind speed with 0° wind-wave misalignment. The fatigue damage obtained using this method is an overestimate, which yields a conservative design (since the damage from all different directions are accumulated in one direction). For the extreme limit state, an Extreme Wind Model (EWM) with a 50-year recurrence period is used. Again, no wind-wave misalignment is considered in this case.

This setup results in 72 simulation scenarios (11 load cases for NTM with 6 random seeds and wind speed bin size of 2, and 1 load case for EMW-50 year with 6 random seeds and wind speed of

[3] United States Department of Labor, Producer Price Indexes, http://www.bls.gov/ppi/, retrieved on 01 November 2013.

50 m/s). In the authors' experience, this is the minimum number of load cases that should be considered to obtain a practical design, as they are the design drivers in most cases. Considering more design load cases using this method is technically possible, but it requires more computational time.

2.3. Practical considerations

There are some issues related to the MDO approach in this research that are unique, and therefore require further explanation.

2.3.1. Multilevel optimization approach

Since this research deals with the simultaneous design optimization of blade and tower, the number of design variables is large. To overcome this problem, a size reduction technique should be employed to enable some computational time savings. An approach where the aerodynamic optimization is performed in sequence with a structural optimization is possible, but this would result in a suboptimal solution Chittick and Martins [55]. Instead, the design variables are decomposed here that results in a bi-level optimization approach as shown in Fig. 4.

In the first level, the blade length, tower height and rated rotational speed are optimized, while all other design variables are fixed. The blade-tip-speed constraint is the only constraint involved here. This setup results in an optimization problem that minimizes LCOE with respect to three design variables subject to one constraint.

After finding the optimum values of the blade length, tower height and rated rotational speed, the second level optimization takes place. In the second level, blade length, tower height and rated rotational speed are fixed and all other design variables are varying. Here, all constraints except the blade-tip-speed constraint are enforced. The objective is to minimize LCOE with respect to 20 design variables subject to 50 design constraints.

The evaluation of the objective function and design constraints takes on average 45 min of wall time for level one, and 30 min for level two. These two levels take place at each global iteration of the optimization process. Parallel computing is used to speed up the optimization process. The evaluation of the objective function and the design constraints requires computations at different wind speeds. In this work each wind speed was run on a separate CPU to enable a faster optimization iteration, and in total 14 parallel computational nodes were used to optimize the design.

2.3.2. Optimization algorithm

Due to the computational expense in computing the objective function and design constraints, a gradient-based algorithm is the best option in this case. For the first level, Convex linearization (CONLIN) is used, which is a first order algorithm Fleury [56]. For the second level of the optimization process, a second order algorithm—the Lagrange Multiplier (LM) method—is used Birgin and Martinez [57]. For both algorithms, the gradients are calculated using the finite-difference method.

The optimization process runs until an acceptable convergence on the objective function with a tolerance of 0.001 is obtained. This tolerance is achieved after 4 iterations of a multilevel optimization, and therefore no further optimization is needed afterward.

It also should be noted that gradient-based optimization has the well-known problem of getting stuck in local minima. Starting the optimization from different point on the design space is an option, but this is not considered in this research, since the aim of this paper is to use this framework and apply that on an existing design and see how it works in practice rather than finding the global minimum.

2.3.3. Wind turbine control strategy

Similar to the 5 MW NREL wind turbine, a VS (Variable-speed) pitch-regulated control concept is used here with the same DLL (Dynamic Link Library) file and parameters. For the below-rated region, a variable-speed strategy is used, where the generator torque controller maximizes the energy output by adjusting the rotational speed. For the above-rated region, active pitch controller strategy is used where the PI (Proportional-integral) controller maintains the power output at 5 MW by pitching the blade into or out of the wind Bianchi et al. [58].

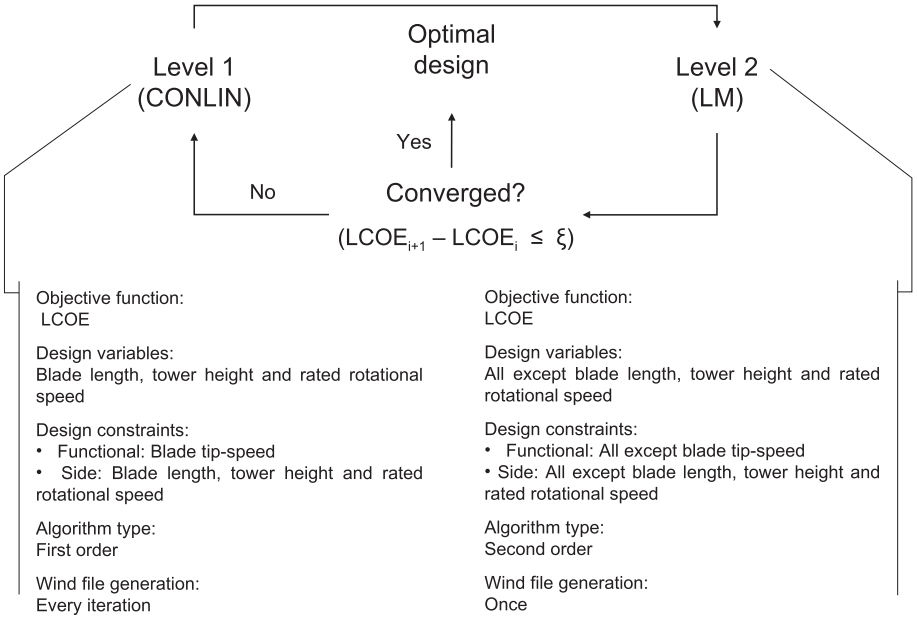

Fig. 4. Multilevel optimization approach of the wind turbine to decompose the design space and speed up the optimization process.

2.3.4. Evaluation of the design constraints

The structural stresses are obtained by converting the load time series from the aeroelastic solver FAST to a stress time series for every wind speed bin from cut-in to cut-out using Crunch. A peak-finding algorithm is used to find the maximum stress that appears as the design constraint. For doing life time fatigue calculation, rain flow cycle counting is applied on the FAST stress time series for every wind speed bin from cut-in to cut-out. Palmgren–Miner's ruler is used to obtain the partial fatigue damage resulting from every wind speed bin, and each partial damage is added to obtain the cumulative fatigue damage.

The natural frequencies are based on the blade and tower mass and stiffness distribution, and are computed using BModes, which is a modal analysis code Bir [47]. The blade-tower clearance is a direct output of FAST. Tip-speed is obtained by multiplying the blade length to the rotor rotational speed for every wind speed from cut-in to cut-out.

3. Results

This section presents the results of the optimized 5 MW NREL wind turbine. The goal of optimizing the NREL wind turbine is to show the potential of the optimization method and understand the design drivers and trends for this type of turbine.

The results are categorized in three parts. First, the optimized gross properties of rotor and tower are presented and compared with the original 5 MW NREL design. Second, the design constraints of the system are presented, with an emphasis on showing the design drivers of the 5 MW optimized turbine. Third, the LCOE contributions from all the elements of the system are analyzed.

3.1. Optimized gross properties

Fig. 5 shows the chord distribution along the NREL and optimized blades. Note that the optimized blade is 3.6% longer than the NREL blade (63.7 m vs. 61.5 m). As the figure shows, in the circular region (station 1 to 3 at the blade root), the optimized blade has slightly smaller diameter than the NREL blade. From the aerodynamic point of view this region does not contribute to power production and the slight decrease can best be explained from structural point of view.

The reason for this reduction is mainly a better distribution of the mass and stiffness along the blade. Although it could be argued that the optimized blade is larger and experiences higher loads, and therefore a larger root diameter is required, it has a lower rated wind speed (because of larger rotor diameter), and that balances out this effect.

The chord of the optimized blade shows an increase after the circular region when compared to the NREL blade, but the difference remains almost constant up to the vicinity of the blade tip.

Fig. 6 shows the twist distributions for the NREL and optimized blades. The twist angle is reduced for the optimized blade outboard of the circular section, but then it matches the NREL blade twist at the tip. This is because of introducing a twist angle of zero at the tip as a hard constraint to be met by the optimizer while interpolating the twist distribution. Therefore, by definition, both the optimized and the NREL blade twist distribution is zero at the tip that is mainly to minimize losses and noise.

Considering the fact that both rotors have a different chord, twist angle, blade length, and rated rotational speed, a one to one comparison is difficult to make. It is the combination of these properties that makes one design better over the other with respect to the objective function.

The blade thickness distribution is used to extract the flapwise and edgewise stiffnesses, and mass per unit length of the blade. The computation of the stiffness and other useful structural properties is based on an analytical model of the blade, using the real geometry and the weight averaging method described by Ashuri et al. [59]. Fig. 7 shows the stiffness distribution along the blade of both designs. The optimized flapwise stiffness is lower near the root, but it increases toward the tip. In the edgewise direction, the optimized blade is generally more flexible than the NREL blade.

The mass per unit length for both the NREL and optimized blades is shown in Fig. 8. The blade mass of the 5 MW NREL wind turbine is 17,740 kg, while the optimized blade has a mass of 18,490 kg, which is 4.2% heavier. This additional mass is partly because the optimized blade is longer. Additionally, the mass distribution of the optimized blade is in general higher than the NREL blade.

Fig. 9 shows the design variables of the optimized tower compared to the NREL tower. The mass and height of the optimized

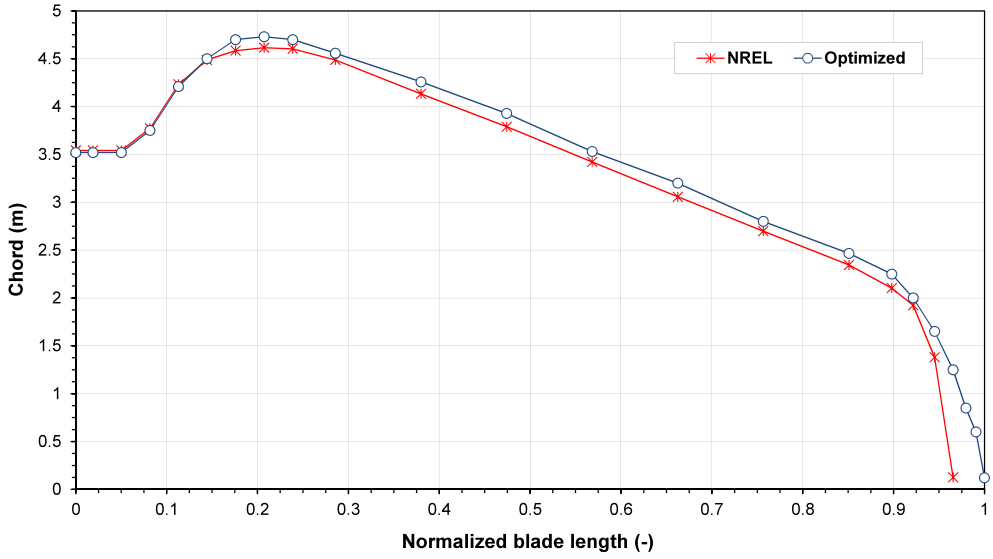

Fig. 5. Chord distribution of the NREL and optimized blades.

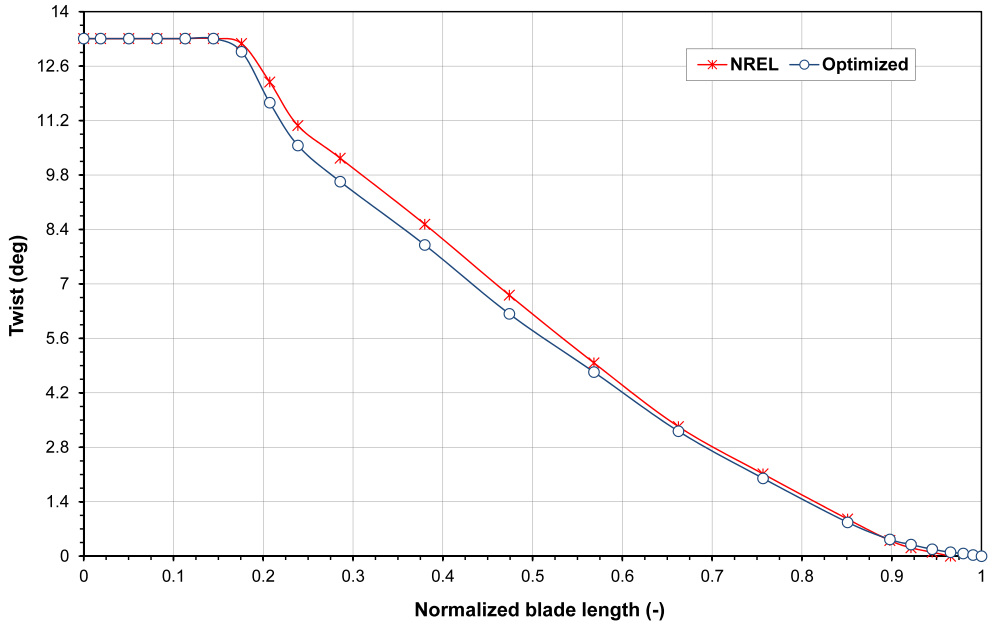

Fig. 6. Twist distribution of the NREL and optimized design along the blade.

tower are 372 tonnes, and 89.8 m, respectively, whereas for the NREL tower these are 347 tonnes and 87.6 m. The optimized tower is higher, to meet the same interface clearance requirement as the NREL tower. This is achieved by defining the bound of the tower and blade lengths in such a way that a minimum desired clearance of 13.5 m from the blade tip (phasing down) to the interface level is maintained.

The optimized wind turbine has a 2.5% higher rated rotational speed relative to the NREL turbine (12.4 rpm for the optimized and 12.1 rpm for the NREL design). The influence of this increased rated rotational speed, together with a larger rotor diameter, results in the higher tip-speed for the optimized rotor. While the NREL rotor has a maximum designed tip-speed of 80 m/s, the optimized design has a tip-speed of 84.6 m/s. This corresponds to a 5.7% increase in the tip-speed of the optimized rotor.

It is well known that for offshore wind turbines, there is a clear potential benefit for higher tip-speeds, since noise is not as much of a concern, and thus offshore turbines are not subject to the 80 m/s noise-related limit of onshore wind turbines Malcolm and Hansen [60], Jamieson [61]. Therefore, it is not surprising to see a higher tip-speed for the optimized wind turbine design, which increases the performance.

However, with increasing tip-speed, the blade solidity usually decreases and this may result in a more flexible blade. Although this can be beneficial for system loads, it is problematic for maintaining the preferred blade-tower-clearance in extreme loading conditions. Therefore, there is an optimum for the tip-speed that is governed by several design considerations. In the design of the optimized 5 MW, it is the blade-tower-clearance that prevents a further decrease in the blade's solidity.

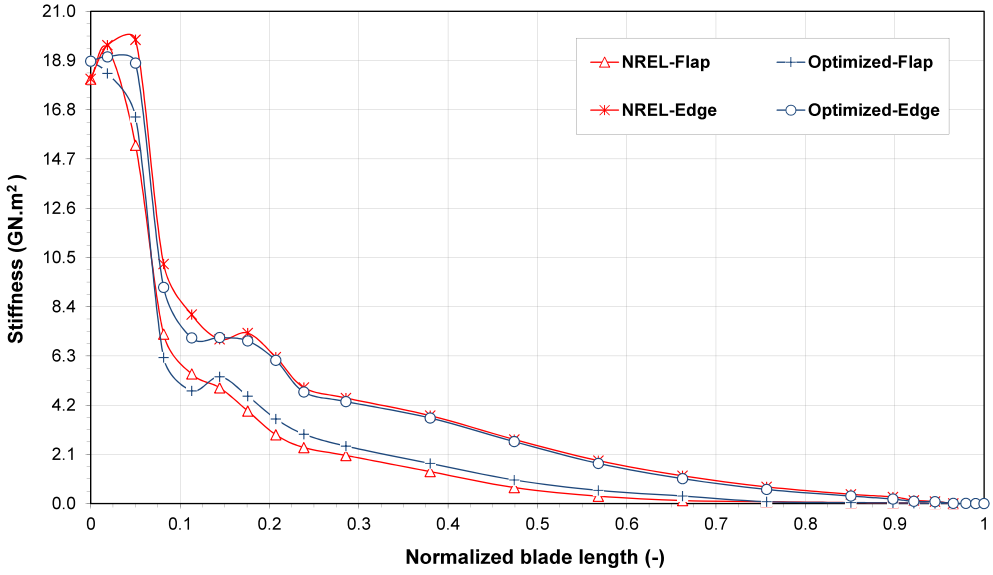

Fig. 7. Stiffness distribution of the NREL and optimized blade.

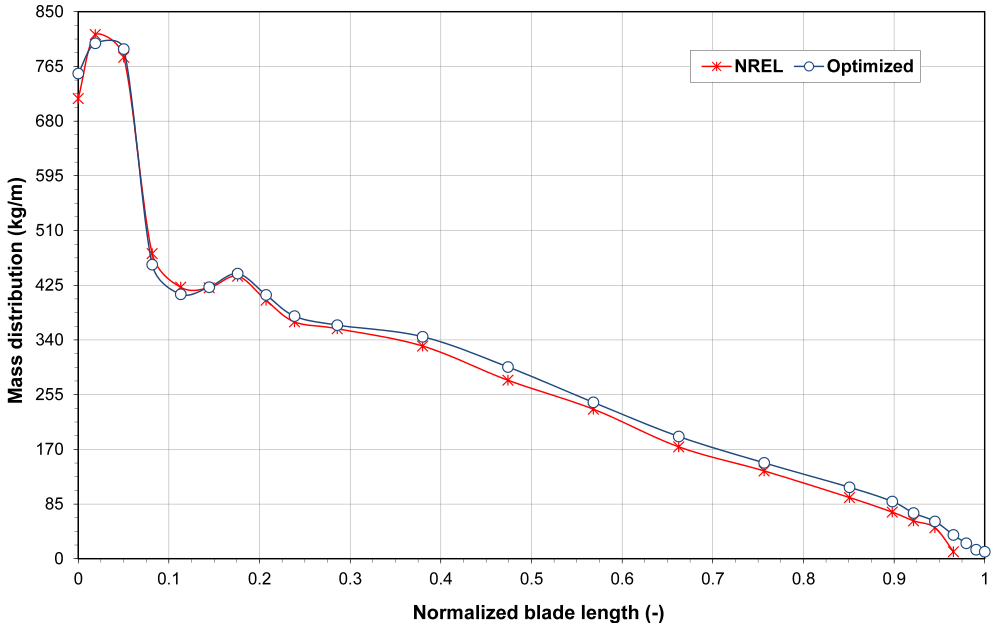

Fig. 8. Mass distribution of the NREL and optimized design along the blade.

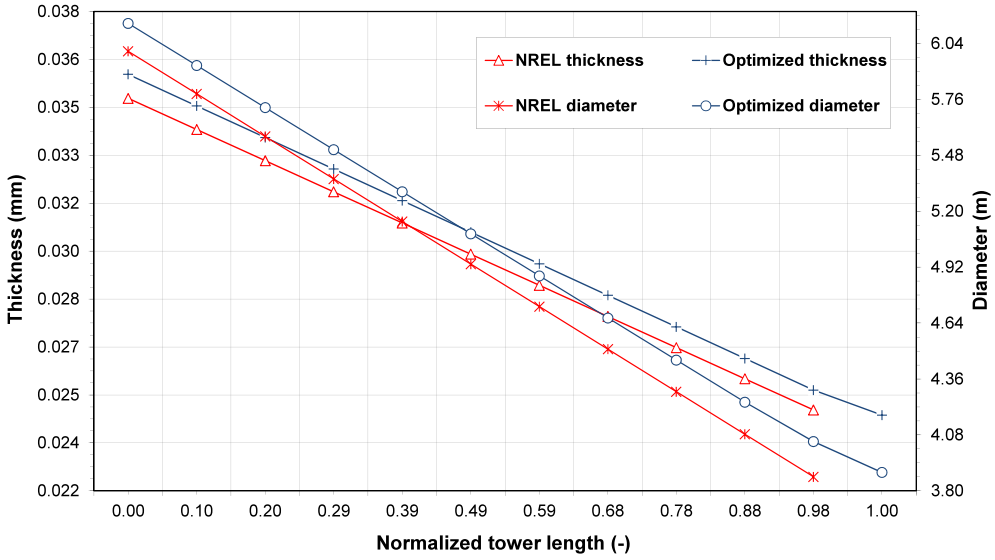

Fig. 9. Thickness and radius distribution of the NREL and optimized design along the tower.

3.2. Design drivers

The design space in which the optimizer searches for the optimum design variables is highly constrained with 51 functional constraints in total as presented before. Therefore, only those constraints that dominate the final design are presented. For the rotor, these active design constraints are the tip-deflection and fatigue. Similarly, fatigue is the highest active design constraint for the tower, which is generally the case for structures subjected to turbulent wind and wave loading.[4]

To have a safe blade-tower-clearance, a lower side constraint for the blade out-of-plane deflection is considered. This is evaluated per iteration and from cut-in to cut-out wind speed, but normally at the rated wind speed the maximum out-of-plane tip-deflection happens that results in the minimum clearance. This is shown in Fig. 10.

As the figure shows, the tip-deflection of the blade reaches a maximum close to the rated wind speed. This peak is due to the high loads that a variable-speed, pitch-regulated wind turbine experiences at the rated wind speed. As the blade pitches above the rated operational point the loads on the blade decrease, resulting in smaller deflections. It should be mentioned that the rated wind speed of the optimized turbine is 11.1 m/s, whereas for the NREL turbine it is 11.4 m/s. The reason for such a change are the differences in blade length, rotor design, and rated rotational speed.

[4] See these references for further consultation: Ashuri et al. [62], van der Meulen et al. [63], Muskulus [64], de Vries et al. [65], Van Der Tempel [66].

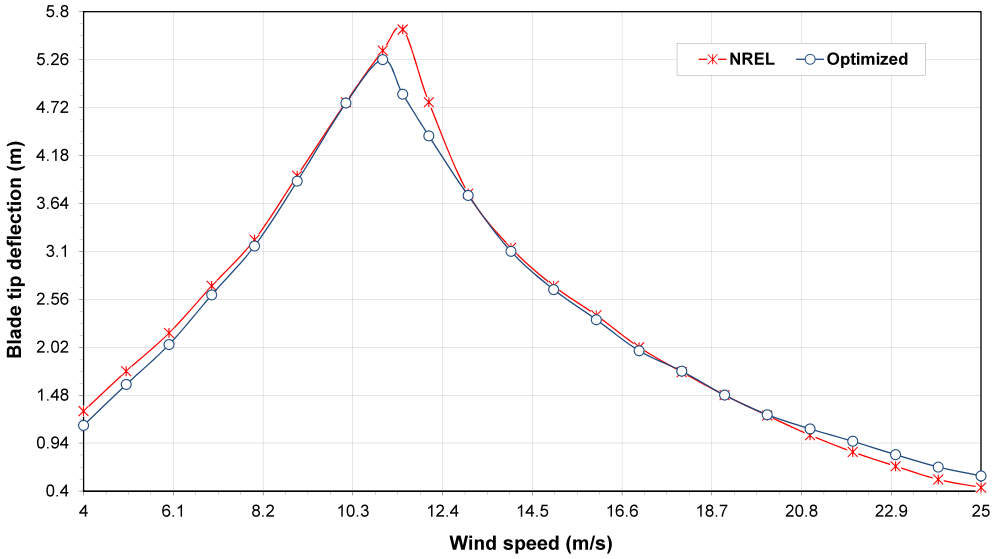

Fig. 10. Blade tip-deflection of the NREL and optimized design at different wind speeds.

The fatigue damage at the root is the maximum in both the flapwise and edgewise directions for both designs compared to other stations. Therefore, only these results are listed in Table 6. As the table shows, the flapwise fatigue damage is higher than the edgewise damage. This demonstrates that the aerodynamic loads are typically higher than the gravity loads for the blade of wind turbines at the 5 MW range size Ashuri and Zaaijer [67], Capponi et al. [68].

The tower fatigue damages is calculated using a similar approach to that of the blade. As seen in Table 7 the side-to-side fatigue damage is much smaller than the fore-aft damage. This is related to the fact that there is no yaw error simulation as a load case in the design process. The addition of a yaw error in the simulation can result in higher side-to-side damage and lower fore-aft damage. Not including a yaw error in the load calculation leads to a more conservative design by making the fore-aft damage the design driver for fatigue.

Despite minor changes in the mass and stiffness distributions of the rotor and tower, the natural frequencies of the optimized design do not show a considerable change relative to the NREL design.

3.3. *Objective function*

To show the effectiveness of the optimization method proposed in this paper a comparison between the 5 MW NREL and the optimized wind turbine is made in Table 8. As the table shows, the cost of energy of the optimized turbine was reduced by 2.3% relative to the NREL one. This reduction is achieved by finding the best match between the system costs and the AEP that results in the minimum LCOE. The optimized wind turbine has a higher ICC, as well as a higher AEP compared to the NREL turbine, but ultimately it yields a lower LCOE, while satisfying all the design constraints.

There are several cost elements with the same value for both wind turbines. These cost elements are either a function of rated power—which is exactly the same for both turbines—or have a fixed value (e.g., the engineering permits needed to construct the site). As an example, the cost model for the foundation is a function of the rated power and valid for a fixed water depth, and since these two parameters are the same for both wind turbines (NREL and the optimized), the cost of foundation remains the same.

4. Discussion and conclusions

For many years, the design of wind turbines was based on a single-discipline or sequential approach Quarton [69]. In this approach, the structural and aerodynamic designs were not performed simultaneously, and components were designed separately. This was mainly due to the complexities of modeling and simulating the interaction among different disciplines, as well as the dynamic interaction between the different components.

Despite many advancements in the last years to develop more sophisticated computational tools to capture the complex physics of the entire wind turbine, most wind turbine design efforts still treat each component separately. Also, few attempts have been made to utilize the integrated MDO approach that is currently implemented in aircraft design Martins et al. [70], Haghighat et al. [71], Kenway and Martins [72].

The research presented herein represents the first design optimization effort that simultaneously designs a wind turbine blade and tower subject to constraints on fatigue, stresses, deflections and frequencies with the LCOE as the objective function. The results show a clear improvement in the quality of the design process by making a realistic assessment of the LCOE and constraints, while preserving the coupling of the components and disciplines, and by taking advantage of the power of numerical optimization.

Table 6
Fatigue damage at the blade root.

Direction	Fatigue cumulative damage (−)
Flap NREL	0.63
Flap optimized	0.70
Edge NREL	0.23
Edge optimized	0.32

Table 7
Fatigue damage at the tower bottom.

Direction	Fatigue cumulative damage (−)
Fore-aft NREL	0.67
Fore-aft optimized	0.69
Side-to-side NREL	0.12
Side-to-side optimized	0.13

Table 8
US Dollar (USD) based cost comparison of the NREL and optimized wind turbines.

Cost component (1000 USD)	NREL	Optimized
Blades	1062.3	1088.4
Hub	130.2	134.4
Pitch mechanism and bearing	242.0	265.2
Nose cone	13.6	14.3
Low speed shaft	166.8	184.3
Main bearings	64.4	72.7
Gearbox	877.2	877.2
Mechanical brake and coupling	11.0	11.0
Generator	398.0	398.0
Power electronics	393.2	393.2
Yaw drive and bearing	146.3	161.2
Main frame	162.7	174.0
Platform and railing	89.5	95.7
Nacelle cover	73.3	73.3
Electrical connections	308.8	308.8
Hydraulic and cooling system	77.2	77.2
Control,safety and condition monitoring	65.3	65.3
Tower	939.1	1005.5
Marinization	561.6	582.6
Turbine capital costs (TCC)	4722.4	4898.5
Foundation system	2174.7	2174.7
Transportation	1568.3	1568.3
Port and staging equipment	144.9	144.9
Turbine installation	732.8	732.8
Electrical interface and connection	2063.5	2063.5
Permits, engineering and site assessment	215.5	215.5
Personnel access equipment	70.2	70.2
Scour protection	403.0	403.0
Decommissioning	362.8	368.1
Balance of station costs (BOS)	7373.2	7373.2
Offshore warranty premium	624.1	647.4
Initial capital cost (ICC)	13,083.0	14,651.0
Levelized replacement costs	99.0	99.0
Operation and maintenance	561.4	585.4
Fixed charge rate	0.1185	0.1185
AEP (GWhr)	23.91	25.19
LCOE (USD/kWhr)	0.0658	0.0643

In this way, a global definition of the objective function, design variables and design constraints for all the disciplines (rather than optimizing the structure for minimum weight and optimizing the aerodynamics for maximum energy output) and the concurrent design of the rotor and tower enables the optimizer find better multidisciplinary design solutions. The use of the integrated methodology contributed to 2.3% reduction in the LCOE compared to the baseline NREL turbine. Therefore, the authors believe that the integrated design methodology is vital for the development of future wind turbines that have to be more optimized than they are today in order to be competitive.

5. Future work

In this research, controller parameters were not part of the design optimization and the authors believe that by including the controller design in the process as an additional discipline would results in a further reduction in the LCOE Ashuri et al. [73]. Adding local and global buckling in the structural design constraints for the blade and tower is an additional recommendation for future work.

To model the sectional properties of the blade, a simplified method was used that did not take into account the bend-twist coupling and the stacking sequence of the composite materials used in the blade. A more sophisticated method to account for these effects is another recommendation for future work.

Finite differences were used to estimate the gradients for the optimization algorithm. By introducing more advanced techniques, such as complex-step variable method Martins et al. [74], and the coupled adjoint method Martins et al. [75], Martins and Hwang [76], Kenway et al. [77], more accurate gradients can be obtained. The adjoint method in particular would significantly reduce the optimization time and enable the optimization with respect to a much larger number of variables.

To make a more realistic design, more design load cases need to be simulated. At the same time, high-performance computing should be used in its full potential to allow the inclusion of these additional load cases.

Acknowledgments

The authors acknowledge the scientific guidance of Professor Anthony Waas, from the Department of Aerospace Engineering of the University of Michigan, Ann Arbor, USA. Funding for doing this research came from the NL Agency, under the frame work of INNWIND project, which is acknowledged.

References

[1] Martins JRRA, Lambe AB. Multidisciplinary design optimization: a survey of architectures. AIAA J 2013;51(9):2049–75. http://dx.doi.org/10.2514/1.J051895.
[2] Beyer HG, Rüger T, Schäfer G, Waldl HP. Optimization of wind farm configurations with variable number of turbines. In: Proceedings European Union Wind Energy Conference, Göteborg; 1996. pp. 1073–6.
[3] Grady SA, Hussaini MY, Abdullah MM. Placement of wind turbines using genetic algorithms. Renew Energy 2005;30(2):259–70.
[4] Castro Mora J, Calero Barón JM, Riquelme Santos JM, Burgos Payán M. An evolutive algorithm for wind farm optimal design. Neurocomputing 2007;70(16):2651–8.
[5] Marmidis G, Lazarou S, Pyrgioti E. Optimal placement of wind turbines in a wind park using Monte Carlo simulation. Renew Energy 2008;33(7):1455–60.
[6] Kusiak A, Song Z. Design of wind farm layout for maximum wind energy capture. Renew Energy 2010;35(3):685–94.
[7] Emami A, Noghreh P. New approach on optimization in placement of wind turbines within wind farm by genetic algorithms. Renew Energy 2010;35(7):1559–64.
[8] Meyers J, Meneveau C. Optimal turbine spacing in fully developed wind farm boundary layers. Wind Energy 2012;15(2):305–17.
[9] Diveux T, Sebastian P, Bernard D, Puiggali JR, Grandidier JY. Horizontal axis wind turbine systems: optimization using genetic algorithms. Wind Energy 2001;4(4):151–71.
[10] Fuglsang P, Thomsen K. Site-specific design optimization of 1.5–2.0 MW wind turbines. J Sol Energy Eng 2001;123(4):296–303.
[11] Benini E, Toffolo A. Optimal design of horizontal-axis wind turbines using blade-element theory and evolutionary computation. J Sol Energy Eng 2002;124(4):357–63.
[12] Maalawi KY, Negm HM. Optimal frequency design of wind turbine blades. J Wind Eng Ind Aerod 2002;90(8):961–86.
[13] Maalawi KY, Badr MA. A practical approach for selecting optimum wind rotors. Renew Energy 2003;28(5):803–22.
[14] Jureczko M, Pawlak M, Mezyk A. Optimisation of wind turbine blades. J Mater Process Technol 2005;167(2):463–71.
[15] Lund E, Stegmann J. On structural optimization of composite shell structures using a discrete constitutive parametrization. Wind Energy 2005;8(1):109–24.
[16] Méndez J, Greiner D. Wind blade chord and twist angle optimization using genetic algorithms. In: Fifth International Conference on Engineering Computational Technology, Las Palmas de Gran Canaria, Spain; 2006. pp. 12–5.
[17] Lee K, Joo W, Kim K, Lee D, Lee K, Park J. Numerical optimization using improvement of the design space feasibility for korean offshore horizontal axis wind turbine blade. In: European Wind Energy Conference and Exhibition EWEC; 2007. pp. 1–8.
[18] Kenway GKW, Martins JRRA. Aerostructural shape optimization of wind turbine blades considering site-specific winds. In: Proceedings of the 12th AIAA/ISSMO Multidisciplinary Analysis and Optimization Conference. Victoria, BC; 2008. pp. 1–12. AIAA 2008-6025.
[19] Xudong W, Shen WZ, Zhu WJ, Sorensen JN,C,J. Shape optimization of wind turbine blades. Wind Energy 2009;12(8):781–803.
[20] Clifton-Smith MJ. Wind turbine blade optimisation with tip loss corrections. Wind Eng 2009;33(5):477–96.
[21] Lee KH, Kim KH, Lee DH, Lee KT, Park JP. Two-step optimization for wind turbine blade with probability approach. J Sol Energy Eng 2010;132(3).
[22] Kwon HI, You JY, Kwon OJ. Enhancement of wind turbine aerodynamic performance by a numerical optimization technique. J Mech Sci Technol 2012;26(2):455–62.
[23] Jeong J, Park K, Jun S, Song K, Lee DH. Design optimization of a wind turbine blade to reduce the fluctuating unsteady aerodynamic load in turbulent wind. J Mech Sci Technol 2012;26(3):827–38.

[24] Bottasso CL, Campagnolo F, Croce A. Multi-disciplinary constrained optimization of wind turbines. Multibody Syst Dyn 2012;27(1):21–53.
[25] Maki K, Sbragio R, Vlahopoulos N. System design of a wind turbine using a multi-level optimization approach. Renew Energy 2012;43(12):101–10.
[26] Negm HM, Maalawi KY. Structural design optimization of wind turbine towers. Comput Struct 2000;74(6):649–66.
[27] Yoshida S. Wind turbine tower optimization method using a genetic algorithm. Wind Eng 2006;30(6):453–69.
[28] Uys PE, Farkas J, Jarmai K, Van Tonder F. Optimisation of a steel tower for a wind turbine structure. Eng Struct 2007;29(7):1337–42.
[29] Silva MA, Arora JS, Brasil RMLRF. Formulations for the optimal design of RC wind turbine towers. In: Internationl Conference on Engineering Optimization; 2008. pp. 1–9.
[30] Karadeniz H, Toğan V, Vrouwenvelder T. An integrated reliability-based design optimization of offshore towers. Reliab Eng Syst Saf 2009;94(10):1510–6.
[31] Petrini F, Manenti S, Gkoumas K, Bontempi F. Structural design and analysis of offshore wind turbines from a system point of view. Wind Eng 2010;34(1):85–108.
[32] Torcinaro M, Petrini F, Arangio S. Structural offshore wind turbines optimization. In: Proceedings of the 12th biennial ASCE Aerospace Division International Conference (Earth & Space 2010), Honolulu, USA; 2010. pp. 2130–42.
[33] Thiry A, Bair F, Buldgen L, Raboni G, Rigo P. Optimization of monopile offshore wind structures. In: International Conference on Marine Structures; 2011. pp. 633–42.
[34] Haghi R, Ashuri T, van der Valk PLC, Molenaar DP. Integrated multidisciplinary constrained optimization of offshore support structures. In: The science of making torque from wind, Oldenburg, Germany; 2012. pp. 1–10.
[35] Zwick D, Muskulus M, Moe G. Iterative optimization approach for the design of full-height lattice towers for offshore wind turbines. Energy Procedia 2012;24:297–304.
[36] Molde H. Simulation-based optimization of lattice support structures for offshore wind energy. MSc thesis. Trondheim, Norway: Norwegian University of Science and Technology; 2012.
[37] Spall JC. An overview of the simultaneous perturbation method for efficient optimization. Johns Hopkins APL Technical Digest 1998;19(4):482–92.
[38] Karpat F. A virtual tool for minimum cost design of a wind turbine tower with ring stiffeners. Energies 2013;6(8):3822–40.
[39] Tegen S, Lantz E, Hand M, Maples B, Smith A, Schwabe P. 2011 cost of wind energy review. Tech. Rep. Golden, Colorado: National Renewable Energy Laboratory; 2013. NREL/TP-5000–56266.
[40] Ashuri T, Zaaijer MB. Review of design concepts, methods and considerations of offshore wind turbines. In: European Offshore Wind Conference and Exhibition, Berlin, Germany; 2007. pp. 1–10.
[41] Jonkman JM, Butterfield S, Musial W, Scott G. Definition of a 5-MW reference wind turbine for offshore system development. Tech. Rep. NREL/TP-500-38060. USA: National Renewable Enrgy Labratory; 2009.
[42] Lambe AB, Martins JRRA. Extensions to the design structure matrix for the description of multidisciplinary design, analysis, and optimization processes. Struct Multidiscip Optim 2012;46:273–84. http://dx.doi.org/10.1007/s00158-012-0763-y.
[43] Jonkman BJ, Buhl ML. Turbsim user's guide. Tech. Rep. Golden, Colorado: National Renewable Energy Laboratory; 2007. NREL/TP-500–41136.
[44] Laino DJ, Hansen AC. User's guide to the wind turbine dynamics aerodynamics computer software AeroDyn. Tech. Rep. Salt Lake City, UT: Windward Engineering LLC; 2002. Prepared for the National Renewable Energy Laboratory under Subcontract No. TCX-9-29209-01.
[45] Viterna LA, Janetzke DC. NASA STI/Recon Technical Report N. Theoretical and experimental power from large horizontal-axis wind turbines, vol. 82; 1982. pp. 33830–9.
[46] Jonkman JM, Buhl ML. Fast user's guide. Tech. Rep. Golden, Colorado: National Renewable Energy Laboratory; 2004. NREL/EL-500–29798
[47] Bir GS. User's guide to BModes. Tech. Rep. Golden, Colorado: National Renewable Energy Laboratory; 2007.
[48] Buhl ML. Crunch user's guide. Tech. Rep. Golden, Colorado: National Renewable Energy Laboratory; 2003. NREL/EL-500-30122.
[49] Fingersh L, Hand M, Laxson A. Wind turbine design cost and scaling model. Tech. Rep. Golden, Colorado: National Renewable Energy Laboratory; 2006. NREL/TP-500-40566.
[50] Frendahl M, Rychlik I. Rainflow analysis: Markov method. Int J fatigue 1993;15(4):265–72.
[51] IEC61400. Wind turbines, part 3: design requirements for offshore wind turbines; 2009.
[52] Miner MA. Cumulative damage in fatigue. J Appl Mech 1945;12(3):159–64.
[53] Ashuri T. Integrated aeroservoelastic design and optimization of large offshore wind turbines. PhD thesis. the Netherlands: Delft University of Technology; 2012.
[54] Brand AJ. Offshore wind atlas of the Dutch part of the North sea. Tech. Rep.; ECN-M-09-050. Petten: Energy research Centre of the Netherlands; 2008.
[55] Chittick IR, Martins JRRA. An asymmetric suboptimization approach to aerostructural optimization. Optim Eng 2009;10(1):133–52. http://dx.doi.org/10.1007/s11081-008-9046-2.
[56] Fleury C. CONLIN: an efficient dual optimizer based on convex approximation concepts. Struct Multidiscip Optim 1989;1(2):81–9.
[57] Birgin EG, Martinez JM. Improving ultimate convergence of an augmented Lagrangian method. Optim Methods Software 2008;23(2):177–95.
[58] Bianchi F, De Battista H, Mantz R. In: Lavoisier, editor. Wind turbine control systems: principles, modelling and gain-scheduling design (advances in industrial control); 2006.
[59] Ashuri T, Zaaijer MB, van Bussel GJW, van Kuik GAM. An analytical model to extract wind turbine blade structural properties for optimization and upscaling studies. In: The science of making torque from wind, Crete, Greece; 2010. pp. 1–7.
[60] Malcolm DJ, Hansen AC. WindPACT turbine rotor design study. Tech. Rep. Golden, Colorado: National Renewable Energy Laboratory; 2002. NREL/SR-500-32495.
[61] Jamieson P. Innovation in wind turbine design. John Wiley and Sons, Ltd; 2011.
[62] Ashuri T, van Bussel GJW, Mieras S. Development and validation of a computational model for design analysis of a novel marine turbine. Wind Energy 2013;16(1):77–90.
[63] van der Meulen MB, Ashuri T, van Bussel GJW, Molenaar DP. Influence of nonlinear irregular waves on the fatigue loads of an offshore wind turbine. In: The Science of Making Torque from Wind, Oldenburg, Germany; 2012. pp. 1–10.
[64] Muskulus M. The full-height lattice tower concept. Energy Procedia 2012;24:371–7.
[65] de Vries W, Vemula NK, Passon P, Fischer T, Kaufer D, Matha D, et al. Final report wp4. 2: support structure concepts for deep water sites. Tech. Rep.; UpWind project; 2011.
[66] Van Der Tempel J. Design of support structures for offshore wind turbines. PhD thesis. the Netherlands: Delft University of Technology; 2006.
[67] Ashuri T, Zaaijer MB. Size effect on wind turbine blade's design drivers. In: European Wind Energy Conference and exhibition, Brussels, Belgium; 2008. pp. 1–6.
[68] Capponi PC, Ashuri T, van Bussel GJW, Kallesøe B. A non-linear upscaling approach for wind turbine blades based on stresses. In: European Wind Energy Conference and Exhibition, Brussels, Belgium. European Academy of Wind Energy; 2011. pp. 1–8.
[69] Quarton DC. The evolution of wind turbine design analysis twenty year progress review. Wind Energy 1998;1(S1):5–24.
[70] Martins JRRA, Alonso JJ, Reuther JJ. High-fidelity aerostructural design optimization of a supersonic business jet. J Aircraft 2004;41(3):523–30.
[71] Haghighat S, Martins JRRA, Liu HHT. Aeroservoelastic design optimization of a flexible wing. J Aircraft 2012;49(2):432–43. http://dx.doi.org/10.2514/1.C031344.
[72] Kenway GKW, Martins JRRA. Multi-point high-fidelity aerostructural optimization of a transport aircraft configuration. J Aircraft 2014;51(1):144–60.
[73] Ashuri T, Zaaijer MB, van Bussel GJW, van Kuik GAM. Controller design automation for aeroservoelastic design optimization of wind turbines. In: The science of making torque from wind, Crete, Greece; 2010. pp. 1–7.
[74] Martins JRRA, Sturdza P, Alonso JJ. The complex-step derivative approximation. ACM Trans Math Software (TOMS) 2003;29(3):245–62. http://dx.doi.org/10.1145/838250.838251.
[75] Martins JRRA, Alonso JJ, Reuther JJ. A coupled-adjoint sensitivity analysis method for high-fidelity aero-structural design. Optim Eng 2005;6(1):33–62. http://dx.doi.org/10.1023/B: OPTE.0000048536.47956.62.
[76] Martins JRRA, Hwang JT. Review and unification of discrete methods for computing derivatives of single- and multi-disciplinary computational models. AIAA J 2013;51(1):2582–99.
[77] Kenway GKW, Kennedy GJ, Martins JRRA. A scalable parallel approach for high-fidelity steady-state aeroelastic analysis and adjoint derivative computations. AIAA J; 2014. http://dx.doi.org/10.2514/1.J052255.